22nd Applied Aerodynamics Conference and Exhibit, August 16-19, 2004, Providence, Rhode Island

Case Studies in Aero-Structural Wing Planform and Section Optimization

Kasidit Leoviriyakit*, and Antony Jameson†
Stanford Univerisity, Stanford, CA, 94305-4035, USA

This paper focuses on aero-structural optimization of wing for long range transport aircraft, using Adjoint based optimization. The paper explores and compares attainable limit such as attainable L/D vs. Mach number, which may be appreciable higher than the historical trend typically used in conceptual design. It also seeks to identify a discernable trend in the planform variables such as sweep, thickness-to-chord ratio, aspect ratio, and chords for optimum wings. Results form wing-fuselage and complete-aircraft-configuration optimizations indicate that by stretching the span together with decreasing sweep and thickening the wing sections the lift-to-drag ratio can be increased without any penalty on the structure weight.

I. Introduction

Most existing airplanes are not truly optimized. They were designed with the analysis and design tools available during the 1970s and 1980s. Design information was mainly provided by the results of analytic theory combined with a fair amount of experimentation. Although analytic theories provided invaluable insight for the design, they usually lacked the accuracy required for the detailed design.

With the advent of the digital computer and the development of fast numerical algorithms, computational methods have increased their role in the airplane design process. Computational Fluid Dynamics (CFD) has been widely used as an aid to analyze the fluid flow, but still not as a direct design tool. The main reason is the number of possible design variations is too large to permit their exhaustive evaluation. Thus it is very unlikely that a truly optimum solution can be found without the assistance of automatic optimization procedures. In order to take full advantage of the possibility of examining a large design space, the numerical simulations need to be combined with automatic search and optimization procedures. This can lead to automatic design methods which will fully realize the potential improvements in aerodynamic efficiency.

In order to find optimum aerodynamic shapes with reasonable computational costs, it pays to regard the wing as a device which controls the flow in order to produce lift with minimum drag. As a result, we can draw on concepts which have been developed in the mathematical theory of control of systems governed by partial differential equations. Using this theory, we can find the Frechet derivative (infinitely dimensional gradient) of the cost function with respect to the shape by solving an adjoint problem, and then we can make an improvement by making a modification in a descent direction. For example, the cost function might be the drag coefficient at a fixed lift, or the lift to drag ratio. During the last decade, this method has been intensively developed, and has proved to be very effective for improving wing section shapes for fixed wing planform.[1,2,3,4,5,6,7,8] Furthermore, this method is not limited to only the wing sections but can be extended to wing planform.

Wing planform modification can yield large improvement in wing aerodynamic performance but can also affect wing weight and stability-and-control characteristics. A pure aerodynamic optimization may lead to highly suspect results because the decrease in drag might come at the expense of the increase in wing weight. Therefore it is essential to account for the effect of planform change on wing weight.

*Doctoral Candidate, Department of Aeronautics and Astronautics, AIAA Member
†Thomas V. Jones Professor of Engineering, Department of Aeronautics and Astronautics, AIAA Member.

The adjoint based optimization method has proved to be very robust. We have applied the method to improve the aerodynamic performance of a variety of wings in transonic flow. Successful examples include wing redesigns for the Boeing 717, Boeing 747, Reno Air Racer, the Falcon 2000, the Gulfstream GIV and GV, and the Embraer 190. The inclusion of planform variation has yielded further improvement of the Boeing 747 wing.

Building on these successes, we believe that the aero-structural wing planform and section optimization can now be used to explore attainable limits such as attainable L/D versus Mach number, which may be appreciably higher than the historical trends typically used in conceptual design. For this purpose we examine a number of case studies, and in particular for the case of long range transport aircraft, we seek to identify any discernable trends in the optimum choice of wing loading, sweep, thickness to chord ratio, and aspect ratio. At the same time these case studies serve to further validate the adjoint based optimization procedure as a robust design tool.

II. Mathematical formulation

The optimization techniques are developed for wing design in viscous compressible flow modeled by the Navier-Stokes equations. The formulation is quit complicated. The detailed derivation can be found in reference.[9] We summarize the formulation here.

In this work the equations of steady flow

$$\frac{\partial f_i}{\partial x_i} - \frac{\partial f_{vi}}{\partial x_i} = 0 \quad \text{in } \mathcal{D},$$

where the state vector w, inviscid flux vector f and viscous flux vector f_v are applied in a fixed computational domain, with coordinates ξ_i, so that

$$\begin{aligned} R(w,S) &= 0 \\ &= \frac{\partial}{\partial \xi_i} F_i - \frac{\partial}{\partial \xi_i} F_{vi} \\ &= \frac{\partial}{\partial \xi_i} S_{ij} f_j - \frac{\partial}{\partial \xi_i} S_{ij} f_{vj} \end{aligned} \tag{1}$$

where S_{ij} are the coefficients of the Jacobian matrix of the transformation. Then geometry changes are represented by changes δS_{ij} in the metric coefficients. Suppose one wishes to minimize the cost function of a boundary integral

$$I = \int_{\mathcal{B}} \mathcal{M}(w,S)\, d\mathcal{B}_\xi + \int_{\mathcal{B}} \mathcal{N}(w,S)\, d\mathcal{B}_\xi \tag{2}$$

where the integral of $\mathcal{M}(w,S)$ could be an aerodynamic cost function, e.g. drag coefficient, and the integral of $\mathcal{N}(w,S)$ could be a structural cost function, e.g. wing weight.

Symbolically, equations (2) and (1) can be represented as a problem of minimizing

$$I = I\left(w,S\right), \tag{3}$$

subject to

$$R\left(w,S\right) = 0. \tag{4}$$

A change in S results in a change

$$\delta I = \left[\frac{\partial I^T}{\partial w}\right] \delta w + \left[\frac{\partial I^T}{\partial S}\right] \delta S, \tag{5}$$

and δw is determined from the equation

$$\delta R = \left[\frac{\partial R}{\partial w}\right] \delta w + \left[\frac{\partial R}{\partial S}\right] \delta S = 0. \tag{6}$$

Generally to completely represent a wing surface, the size of the design parameter S is in the order of four thousand. If we were to follow the traditional way of calculating gradient using the finite difference, it would require us to solve equation (6) about four thousand times, which is extremely expensive to solve.

In order to reduce the computational costs, it turns out that there are advantages in formulating the problems within the framework of the mathematical theory for the control of systems governed by partial differential equations.[10] A wing, for example, is a device to produce lift by controlling the flow, and its design can be regarded as a problem in the optimal control of the flow equations by variation of the shape of the boundary.

Using techniques of control theory, the gradient can be determined indirectly by solving an adjoint equation which has coefficients defined by the solution of the flow equations. The cost of solving the adjoint equation is comparable to that of solving the flow equations. Thus the gradient can be determined with roughly the computational costs of two flow solutions, independently of the number of design variables, which may be infinite if the boundary is regarded as a free surface.

The underlying concepts are clarified by the following abstract description of the adjoint method. Recall equations (5) and (6). Since the variation δR is zero, it can be multiplied by a Lagrange Multiplier ψ and subtracted from the variation δI without changing the result. Thus equation (5) can be replaced by

$$\begin{aligned} \delta I &= \frac{\partial I^T}{\partial w}\delta w + \frac{\partial I^T}{\partial S}\delta S - \psi^T\left(\left[\frac{\partial R}{\partial w}\right]\delta w + \left[\frac{\partial R}{\partial S}\right]\delta S\right) \\ &= \left\{\frac{\partial I^T}{\partial w} - \psi^T\left[\frac{\partial R}{\partial w}\right]\right\}\delta w + \left\{\frac{\partial I^T}{\partial S} - \psi^T\left[\frac{\partial R}{\partial S}\right]\right\}\delta S. \end{aligned} \tag{7}$$

Choosing ψ to satisfy the adjoint equation,

$$\left[\frac{\partial R}{\partial w}\right]^T \psi = \frac{\partial I}{\partial w}, \tag{8}$$

the first term is eliminated, and we find that

$$\delta I = \mathcal{G}\delta S, \tag{9}$$

where

$$\mathcal{G} = \frac{\partial I^T}{\partial S} - \psi^T\left[\frac{\partial R}{\partial S}\right].$$

The advantage is that equation (9) is independent of δw, with the result that the gradient of I with respect to an arbitrary number of design variables can be determined without the need for additional flow-field evaluations.

Note that equation (4) is a partial differential equation. Thus the adjoint equation (8) is also a partial differential equation and determination of the appropriate boundary conditions requires careful mathematical treatment. For instant the inviscid boundary condition of (2) is

$$n_i\psi^T S_{ij} f_{j_w} = \mathcal{M}_w + \mathcal{N}_w, \tag{10}$$

where $\mathcal{M}_w = \frac{\partial \mathcal{M}}{\partial w}$, and $\mathcal{N}_w = \frac{\partial \mathcal{N}}{\partial w}$.

Once equation (9) is established, an improvement can be made with a shape change

$$\delta S = -\lambda\mathcal{G}$$

where λ is positive, and small enough that the first variation is an accurate estimate of δI. The variation in the cost function then becomes

$$\delta I = -\lambda\mathcal{G}^T\mathcal{G} < 0.$$

After making such a modification, the gradient can be recalculated and the process repeated to follow a path of steepest descent until a minimum is reached. In order to avoid violating constraints, such as a minimum acceptable wing thickness, the gradient may be projected into an allowable subspace within which the constraints are satisfied. In this way, procedures can be devised which must necessarily converge at least to a local minimum.

In fact the gradient $\mathcal{G}$ is generally of a lower smoothness class than the shape S. Hence it is important to restore the smoothness. This may be effected by passing to a weighted Sobolev inner product of the form

$$\langle u, v\rangle = \int (uv + \epsilon\frac{\partial u}{\partial \xi}\frac{\partial v}{\partial \xi})\, d\xi$$

This is equivalent to replacing $\mathcal{G}$ by $\bar{\mathcal{G}}$, where in one dimension

$$\bar{\mathcal{G}} - \frac{\partial}{\partial \xi}\epsilon\frac{\partial \bar{\mathcal{G}}}{\partial \xi} = \mathcal{G}, \quad \bar{\mathcal{G}} = \text{zero at end points}$$

and making a shape change $\delta S = -\lambda\bar{\mathcal{G}}$.

III. Implementation

A. Planform design variables

In this work, we model the wing of interest using six planform variables: root chord (c_1), mid-span chord (c_2), tip chord (c_3), span (b), sweepback(Λ), and wing thickness ratio (t), as shown in figure 1. This choice of

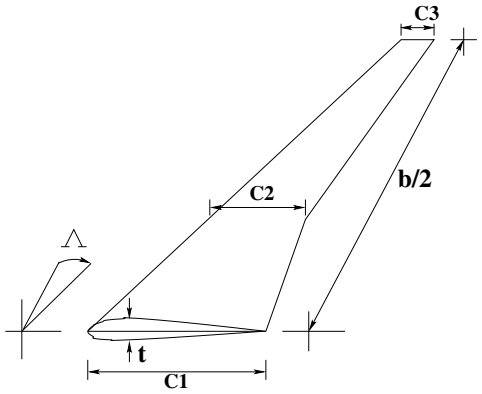

Figure 1. Modeled wing governed by six planform variables; root chord (c_1), mid-span chord (c_2), tip chord (c_3), span (b), and sweepback(Λ), wing thickness ratio (t).

design parameters will lead to an optimum wing shape that will not require an extensive structural analysis and can be manufactured effectively.

B. Cost function for planform design

In order to design a high performance transonic wing, which will lead to a desired pressure distribution, and still maintain a realistic shape, the natural choice is to set

$$I = \alpha_1 C_D + \alpha_2 \frac{1}{2}\int_{\mathcal{B}} (p - p_d)^2 dS + \alpha_3 C_W \tag{11}$$

with

$$C_W \equiv \frac{\mathcal{W}_{wing}}{q_\infty S_{ref}} \tag{12}$$

where

C_D	=	drag coefficient,
C_W	=	normalized wing structural weight,
p	=	current surface pressure,
p_d	=	desired pressure,
q_∞	=	dynamic pressure,
S_{ref}	=	reference area,
$\mathcal{W}_{wing}$	=	wing structural weight, and
α_1, α_2, α_3	=	weighting parameters for drag, inverse design, and structural weight respectively.

The constant α_2 is introduced to provide the designer some control over the pressure distribution.

C. Structural weight model

To estimate $\mathcal{W}_{wing}$, a realistic model should account for both planform geometry and wing loading, but it should be simplified enough that we can express it as an analytical function.

An analytical model to estimate the minimal material to resist material and buckling failures has been developed by Wakayama.[11] When shear and buckling effects are small, they may be neglected, resulting in a simplified model developed by Kroo.[12] In this paper, we follow the analysis developed by Kroo.

The wing structure is modeled by a structure box, whose major structural material is the box skin. The skin thickness (t_s) varies along the span and resists the bending moment caused by the wing lift. Then, the structural wing weight can be calculated based on material of the skin.

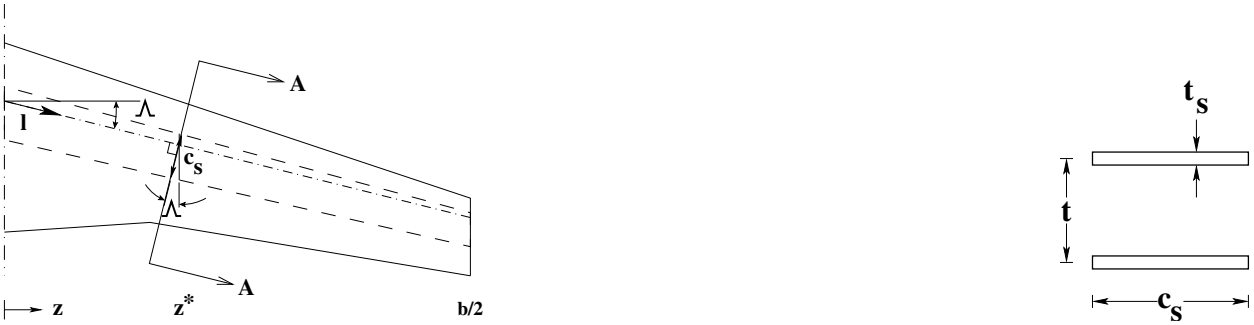

(a) swept wing planform

(b) section A-A

Figure 2. Structural model for a swept wing

Consider a box structure of a swept wing whose quarter-chord swept is Λ and its cross-section A-A as shown in figures 2. The skin thickness t_s, structure box chord c_s, and overall thickness t vary along the span. The maximum normal stress from the bending moment at a section Z^* is

$$\sigma = \frac{M(z^*)}{tt_s c_s}$$

The corresponding wing structural weight is

$$\begin{aligned} \mathcal{W}_{wing} &\propto \int_{structual\ span} \frac{M}{t} dl \\ &= 2\frac{\rho_{mat} g}{\sigma cos(\Lambda)} \int_{-\frac{b}{2}}^{\frac{b}{2}} \frac{M(z^*)}{t(z^*)} dz^* \\ &= 4\frac{\rho_{mat} g}{\sigma cos(\Lambda)} \int_{0}^{\frac{b}{2}} \frac{M(z^*)}{t(z^*)} dz^*, \end{aligned}$$

and

$$C_W = \frac{\beta}{cos(\Lambda)} \int_0^{\frac{b}{2}} \frac{M(z^*)}{t(z^*)} dz^*, \tag{13}$$

where

$$\beta = \frac{4\rho_{mat} g}{\sigma q_\infty S_{ref}},$$

ρ_{mat} is the material density, and g is the gravitational constant.

The bending moment can be calculated by integrating pressure toward the wing tip.

$$\begin{aligned} M(z^*) &= -\int_{z^*}^{\frac{b}{2}} \frac{p(x,z)(z-z^*)}{cos(\Lambda)} dA \\ &= -\int_{z^*}^{\frac{b}{2}} \oint_{wing} \frac{p(x,z)(z-z^*)}{cos(\Lambda)} dx dz \end{aligned}$$

Thus

$$C_W = \frac{-\beta}{cos(\Lambda)^2} \int_0^{\frac{b}{2}} \int_{z^*}^{\frac{b}{2}} \oint_{wing} \frac{p(x,z)(z-z^*)}{t(z^*)} dx dz dz^* \tag{14}$$

To form the corresponding adjoint boundary condition (10), C_W must be expressed as $\int_{\mathcal{B}} d\mathcal{B}_\xi$ in the computational domain, or $\int\int dxdz$ in a physical domain to match the boundary term of (10).

To switch the order of integral of (14), introduce a Heaviside function

$$H(z-z^*) = \begin{cases} 0, & z < z^* \\ 1, & z > z^* \end{cases}$$

Then (14) can be rewritten as

$$\begin{aligned} C_W &= \frac{-\beta}{cos(\Lambda)^2} \cdot \\ &\quad \int_0^{\frac{b}{2}} \int_0^{\frac{b}{2}} \oint_{wing} \frac{p(x,z)H(z-z^*)(z-z^*)}{t(z^*)} dx dz dz^* \\ &= \frac{-\beta}{cos(\Lambda)^2} \int_0^{\frac{b}{2}} \oint_{wing} p(x,z)K(z) dx dz, \end{aligned} \tag{15}$$

where

$$\begin{aligned} K(z) &= \int_0^{\frac{b}{2}} \frac{H(z-z^*)(z-z^*)}{t(z^*)} dz^* \\ &= \int_0^{z} \frac{z-z^*}{t(z^*)} dz^* \end{aligned}$$

In the computational domain,

$$C_W = \frac{-\beta}{cos(\Lambda)^2} \oint_{\mathcal{B}} p(\xi_1, \xi_3) K(\xi_3) S_{22} d\xi_1 d\xi_3, \tag{16}$$

and $K(\xi_3)$ is a one-to-one mapping of $K(z)$.

D. Adjoint boundary condition for the structural weight

For simplicity, it is assumed that the portion of the boundary that undergoes shape modifications is restricted to the coordinate $\xi_2 = 0$. Then (10) may be simplified by incorporating the conditions

$$n_1 = n_3 = 0, \quad n_2 = 1 \quad and \quad d\mathcal{B}_\xi = d\xi_1 d\xi_3,$$

so that the only variation δF_2 needs to be considered at the wall boundary. Moreover, the condition that there is no flow through the wall boundary at $\xi_2 = 0$ is equivalent to

$$U_2 = 0,$$

and

$$\delta U_2 = 0$$

when the boundary shape is modified. Consequently,

$$\delta F_2 = \delta p \begin{Bmatrix} 0 \\ S_{21} \\ S_{22} \\ S_{23} \\ 0 \end{Bmatrix} + p \begin{Bmatrix} 0 \\ \delta S_{21} \\ \delta S_{22} \\ \delta S_{23} \\ 0 \end{Bmatrix}. \tag{17}$$

The variation of C_W is

$$\delta C_W = -\beta \oint_{\mathcal{B}} \delta p \frac{K S_{22}}{cos(\Lambda)^2} + p\delta \left(\frac{K S_{22}}{cos(\Lambda)^2} \right) d\xi_1 d\xi_3, \tag{18}$$

Since δF_2 and δC_W depend only on the pressure, it allows a complete cancellation of dependency of the boundary integral on δp, and the adjoint boundary condition reduces to

$$\psi_2 S_{21} + \psi_3 S_{22} + \psi_4 S_{23} = \frac{-\beta}{cos(\Lambda)^2} K S_{22} \tag{19}$$

E. Gradient calculation for planform variables

The adjoint-based gradient calculation for the wing planform variables has been studied and validated by Leoviriyakit and Jameson.[13,14,15] We include here for completeness.

Consider the variation of the cost function (11)

$$\delta I = \int_{\mathcal{B}} (\delta \mathcal{M} \ + \ \delta \mathcal{N}) \ d\mathcal{B}_\xi + \int_{\mathcal{D}} \psi^T \delta R \, d\mathcal{D}_\xi$$

This can be split as

$$\delta I = [I_w]_I \, \delta w + \delta I_{II}$$

with

$$\delta \mathcal{M} = [\mathcal{M}_w]_I \delta w + \delta \mathcal{M}_{II}$$

and

$$\delta \mathcal{N} = [\mathcal{N}_w]_I \delta w + \delta \mathcal{N}_{II}$$

where the subscripts I and II are used to distinguish between the contributions associated with variation of the flow solution δw and those associated with the metric variations δS. Thus $[\mathcal{M}_w]_I$ represents $\frac{\partial \mathcal{M}}{\partial w}$ with the metrics fixed. Note that δR is intentionally kept unsplit for programming purposes. If one chooses ψ as ψ^*, where ψ^* satisfies

$$(S_{ij} \frac{\partial f_j}{\partial w})^T \frac{\partial \psi^*}{\partial \xi_i} = 0,$$

then

$$\begin{aligned}
\delta I(w, S) &= \delta I(S) \\
&= \int_{\mathcal{B}} (\delta \mathcal{M}_{II} + \delta \mathcal{N}_{II}) \ d\mathcal{B}_\xi + \int_{\mathcal{D}} {\psi^*}^T \delta R \, d\mathcal{D}_\xi \\
&\approx \sum_{\mathcal{B}} (\delta \mathcal{M}_{II} + \delta \mathcal{N}_{II}) \, \Delta \mathcal{B} + \sum_{\mathcal{D}} {\psi^*}^T \Delta \bar{R} \\
&\approx \sum_{\mathcal{B}} (\delta \mathcal{M}_{II} + \delta \mathcal{N}_{II}) \, \Delta \mathcal{B} \\
&+ \sum_{\mathcal{D}} {\psi^*}^T \left(\bar{R}|_{S+\delta S} - \bar{R}|_S \right),
\end{aligned}$$

where $\bar{R}|_S$ and $\bar{R}|_{S+\delta S}$ are volume weighted residuals calculated at the original mesh and at the mesh perturbed in the design direction.

Provided that ψ^* has already been calculated and $\bar{R}$ can be easily calculated, the gradient of the planform variables can be computed effectively by first perturbing all the mesh points along the direction of interest. For example, to calculate the gradient with respect to the sweepback, move all the points on the wing surface as if the wing were pushed backward and also move all other associated points in the computational domain to match the new location of points on the wing. Then re-calculate the residual value and subtract the previous residual value from the new value to form $\Delta \bar{R}$. Finally, to calculate the planform gradient, multiply $\Delta \bar{R}$ by the costate vector and add the contribution from the boundary terms.

This way of calculating the planform gradient exploits the full benefit of knowing the value of adjoint variables ψ^* with no extra cost of flow or adjoint calculations.

F. Choice of weighting constants

1. Maximizing range of the aircraft

The choice of α_1 and α_3 greatly affects the optimum shape. If $\frac{\alpha_3}{\alpha_1}$ is high enough, the optimum shape will have lower C_D and higher C_W than another optimum shape with lower $\frac{\alpha_3}{\alpha_1}$ value.

Leoviriyakit and Jameson[13] propose an intuitive choice of α_1 and α_3 by equating a problem of maximizing range of an aircraft to a problem of minimizing the cost function

$$I = C_D + \frac{\alpha_3}{\alpha_1} C_W.$$

If the simplified Breguet range equation can be expressed as

$$R = \frac{V}{C}\frac{L}{D} log \frac{W_1}{W_2}$$

where C is specific fuel consumption, D is drag, L is lift, R is range, V is aircraft velocity, W_1 is take off weight, and W_2 is landing weight, then choosing

$$\frac{\alpha_3}{\alpha_1} = \frac{C_D}{C_{W_2} log \frac{C_{W_1}}{C_{W_2}}}, \tag{20}$$

corresponds to maximizing the range of the aircraft.

IV. Results

A. Redesign of the Boeing 747 wing

We present a result to show that the optimization can successfully trade planform parameters. We also demonstrate how to apply strategy game theory to the gradient based optimization.

Here, the case chosen is the Boeing 747 wing fuselage combination at Mach 0.87 and a lift coefficient $C_L = 0.42$. The computational mesh is shown in figure 3.

In this test case, the Mach number is the current normal cruising Mach number of 0.85. We allowed section changes together with variations of sweep angle, span length, chords, and section thickness. Figure 4(a) shows the baseline wing. Figure 4(b) shows the redesigned wing. The parameter $\frac{\alpha_3}{\alpha_1}$ was chosen according to formula (20) such that the cost function corresponds to maximizing the range of the aircraft. Here in 30 design iterations the drag was reduced from 137 counts to 117 counts and the structural weight was reduced from 498 counts (80,480 lbs) to 464 counts (75,000 lbs). The large reduction in drag is the result of the increase in span from 212.4 ft to 231.7 ft, which reduces the induced drag. The redesigned geometry also has a lower sweep angle and a thicker wing section in the inboard part of the wing, which both reduce the structural weight. Moreover the section modification prevents the formation of shock. The baseline and optimized planforms are shown in figure 4(c). Overall, the redesign with variation planform gives improvements in both aerodynamic performance and structural weight, compared to the previous optimization with a fixed planform.

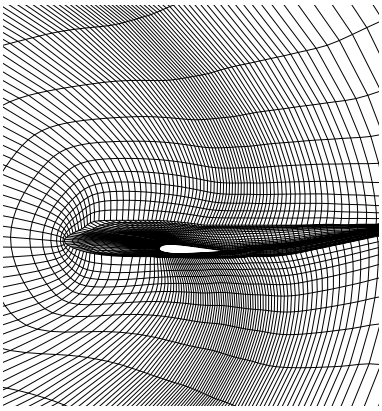

Figure 3. Computational grid of the B747 wing fuselage

B. Redesign of the McDonnell Douglas MD-11 wing

To validate the trend suggested form the previous test case, we select another airplane in a long-range transportation category. Here the case chosen is the MD11 wing fuselage combination at cruising Mach 0.83 and a lift coefficient $C_L = 0.50$.

The baseline and optimized wings are shown in figures 5(a) and 5(b) respectively. Again, the parameter $\frac{\alpha_3}{\alpha_1}$ was chosen to maximizing the range of the aircraft.

In 30 design iterations the drag was reduced from 180 counts to 164 counts, while the wing weight was slightly reduced from 346 counts (33,360 lbs) to 343 (33,090 lbs). Span increases from 174.4 ft to 184.2 ft, sweep slightly reduced from 37.9 to 36.9 degrees, and the section thickness increases. The increase of span reduces vortex drag while the decrease of sweep and the increase of section depth reduce the structural weight.

Both results from Boeing 747 and MD 11 suggest a similar trend to yield large drag reduction, while maintaining low structural weight;

- Increase wing span to reduce vortex drag,
- Reduce sweep but increase section-thickness to reduce structural weight,
- Use section optimization to minimize shock drag.

Although the suggested trend tends to increase the wing area, which increases the skin friction drag, the pressure drag drops faster, dominating the trade-off. Overall, the combined effects yield improvements in both drag and weight.

C. Redesign of the BAe MDO DATUM wing

To further validate this planform-and-section trend, we select BAe MDO DATUM wing. At its cruising Mach .85, this wing has low sweep angle and high thickness-to-chord ratio sections.

This test case presents a technical challenge to the optimization because the BAe and B747 are designed to operate at the same flight condition and their planform are sized closely in the same range. However the original sweep of BAe is already smaller than the optimum sweep of B747 and its wing span is already longer than the optimum span of B747.

Figures 6(a), 6(b), and 6(c) show the original wing, optimized wing, and their planforms respectively. Despite of low-sweep, long-span, and thick-wing-sections of the original wing, the optimal wing has less sweep, longer span, and thicker wing sections. But the changes in the planform are not large. With these changes, the optimum wing shows improvement in both drag and weight. The drag is reduced from 164 counts to 145 counts, and the weight is reduced from 480 counts (87,560 lbs) to 476 counts (86,980 lbs). This optimized BAe wing strongly agree with the trend suggested from the B747 and MD11 cases.

D. Shape optimization of transonic business jet

Aerodynamic shape optimization has been successfully performed for a variety of complex configurations using multi-block structured meshes.[16,17] Meshes of this type can be relatively easily deformed to accommodate shape variations required in the redesign. However, it is both extremely time-consuming and expensive in human costs to generate such meshes. Consequently it may be essential to develop shape optimization methods which use unstructured meshes for the flow simulation.

To emphasize the advantage of unstructured grids for shape optimization, in this section we present results obtained on a complete aircraft configuration. The result form this section can be used to identify the influence of engines and pylons on the redesigned airfoil section.

1. Falcon

As a representative example we show redesigns of a transonic business jet to improve its lift to drag ratio during cruise. As shown in figure 7, the outboard sections of the wing have a strong shock while flying at cruise conditions ($M_\infty = 0.80$, $\alpha = 2^o$). The results of a drag minimization that aims to remove the shocks on the wing are shown in figure 8. The drag has been reduced from 235 counts to 215 counts in about 8 design cycles. The lift was constrained at 0.4 by perturbing the angle of attack. Further, the original thickness of the wing was maintained during the design process ensuring that fuel volume and structural integrity will be maintained by the redesigned shape. The entire design process typically takes about 4 hours on a 1.7 Ghz Athlon processor with 1 Gb of memory. Parallel implementation of the design procedure has also been developed that further reduces the computational cost of this design process.

Figures 7 and 8 also show that the shape modification needed to remove the shock is quite small. Moreover the airfoil sections have similar characteristic to those obtained in sections A and B. This similarity indicates that the effect of engines and pylons on the redesigned airfoil section is not significant. As a result the we

can employ the design procedure similar to the those in the previous sections to improve the performance of a complete-configuration-aircraft.

E. Super wing: Super B747

The results from sections A, B, and C suggest that in general one can improve existing wing performance by reducing the sweep, stretching the span. They also show the benefit of a wing section that has high thickness-to-chord ratio and shock-free pressure profile. Following the trends in planform and airfoil-sections, we now propose to combine them to produce an alternate description of wing for the B747.

In order to explore the limits of attainable performance the B747 wing has been replaced by a completely new wing to produce a "Super B747". An initial design was created by blending supercritical wing sections obtained from other optimizations to the optimum planform which was found in the planform study described in the previous section. Then the RANS optimization code Syn107 was used to obtain minimize drag over 3 design points at Mach .78, .85, and .87, shown in figures 9(a)- 9(c) with a fixed lift coefficient of .45 for the exposed wing, corresponding to a lift coefficient of about .52 when the fuselage lift is included. Because the new wing sections are significantly thicker, the new wing is estimated to be 12,000 pounds lighter than the baseline B747 wing as shown in table 1. At the same time the drag is reduced over the entire range from Mach .78 to .90 with a maximum benefit of 25 counts at Mach .87, as shown in figure 9(d). Figure 10 and table 2 display the lift-drag polar at Mach .86. The drag coefficient of the Super B747 is 142 counts at a lift coefficient of .5, whereas the baseline B747 has the same drag at a lift coefficient of .45. This represents improvement in L/D of more than 10 percent. In combination with the reduction in wing weight and an increase in fuel volume due to the thicker wing section, this should lead to an increase in range which is substantially more than 10 percent.

Table 1. Comparison between Baseline B747 and Super B747 at Mach .86

	C_L	C_D counts	C_W counts
Boeing 747	.45	141.3 (107.0 pressure, 34.3 viscous)	499 (82,550 lbs)
Super B747	.50	141.9 (104.8 pressure, 37.1 viscous)	427 (70,620 lbs)

V. Conclusion

Case studies of wing planform optimization of long range transport aircraft suggest the possibility of extending the attainable lift-to-drag ratio versus Mach number beyond historical trends. They indicate that by stretching the span together with decreasing sweep and thickening the wing sections, the lift-to-drag ratio can be increased without any penalty on the structure weight. Since the influence of engines and pylons on the wing section and planform is not significant, this trend can be extended the optimization in a complete aircraft configurations. While optimization techniques can be used for the rapid identification of optimum wing planform choices in the preliminary design of conventional aircraft, their intelligent exploration may ultimately have an even greater impact by enabling the exploration of radical departures from conventional designs. Case studies are also important for establishing new trends on attainable limit which can serve as a guide for conceptual design. Finally, the optimization method reaches a local optimum which depends on the initial geometry. This is confirmed by the superior performance of the Superb747, which is the result of starting the optimization with a very good initial design.

VI. Acknowledgment

This work has benefited greatly from the support of the Air Force Office of Science Research under grant No. AF F49620-98-1-2004. We would also like to thank Sriram of assistance in obtaining solutions for the Falcon geometry.

References

[1]Jameson, A., "Aerodynamic Design via Control Theory," *Journal of Scientific Computing*, Vol. 3, 1988, pp. 233–260.

[2]Jameson, A., "Computational Aerodynamics for Aircraft Design," *Science*, Vol. 245, 1989, pp. 361–371.

[3]Jameson, A., Martinelli, L., and Pierce, N. A., "Optimum Aerodynamic Design Using the Navier-Stokes Equations," *Theoretical and Computational Fluid Dynamics*, Vol. 10, 1998, pp. 213–237.

[4]Jameson, A., "A perspective on computational algorithms for aerodynamic analysis and design," *Progress in Aerospace Sciences*, Vol. 37, 2001, pp. 197–243.

[5]Jameson, A. and Martinelli, L., "Aerodynamic Shape Optimization Techniques Based on Control Theory," Tech. rep., CIME (International Mathematical Summer Center), Martina Franca, Italy, 1999.

[6]Vassberg, J. C. and Jameson, A., "Computational Fluid Dynamics for Aerodynamic Design: Its Current and Future Impact," *AIAA paper 2001-0538*, AIAA 39th Aerospace Sciences Meeting & Exhibit, Reno, NV, January 2001.

[7]Vassberg, J. C. and Jameson, A., "Aerodynamic Shape Optimization of a Reno Race Plane," *International Journal of Vehicle Design*, Vol. 28, 2002, pp. 318–338.

[8]Kim, S., Alonso, J. J., and Jameson, A., "Design Optimization of High-Lift Configurations Using a Viscous Continuous Adjoint Method," *AIAA paper 2002-0844*, AIAA 40th Aerospace Sciences Meeting & Exhibit, Reno, NV, January 2002.

[9]Leoviriyakit, K., Kim, S., and Jameson, A., "Aero-Structural Wing Planform Optimization Using the Navier-Stokes Equations," *AIAA paper 2004-4479*, 10th AIAA/ISSMO Multidisciplinary Analysis and Optimization Conference, Albany, New York, August 30 - September 1 2004.

[10]Lions, J., *Optimal Control of Systems Governed by Partial Differential Equations*, Springer-Verlag, New York, 1971, Translated by S.K. Mitter.

[11]Wakayama, S., "Lifting Surface Design Using Multidisplinary Optimization," Tech. rep., Stanford University Doctoral Dissertation, Stanford, CA, 1994.

[12]Kroo, I. M., "Design and Analysis of Optimally-Loaded Lifting Systems," *AIAA paper 1984-2507*, October 1984.

[13]Leoviriyakit, K. and Jameson, A., "Aerodynamic Shape Optimization of Wings including Planform Variables," *AIAA paper 2003-0210*, 41st Aerospace Sciences Meeting & Exhibit, Reno, Nevada, January 2003.

[14]Leoviriyakit, K., Kim, S., and Jameson, A., "Viscous Aerodynamic Shape Optimization of Wings including Planform Variables," *AIAA paper 2003-3498*, 21st Applied Aerodynamics Conference, Orlando, Florida, June 2003.

[15]Leoviriyakit, K. and Jameson, A., "Aero-Structural Wing Planform Optimization," *AIAA paper 2004-0029*, 42nd Aerospace Sciences Meeting & Exhibit, Reno, Nevada, January 2004.

[16]Reuther, J., Jameson, A., Alonso, J. J., Rimlinger, M. J., and Saunders, D., "Constrained Multipoint Aerodynamic Shape Optimization Using an Adjoint Formulation and Parallel Computers," *AIAA paper 97-0103*, 35th Aerospace Sciences Meeting and Exhibit, Reno, Nevada, January 1997.

[17]Cliff, S., Reuther, J., Sanders, D., and Hicks, R., "Single and Multipoint Aerodynamic Shape Optimization of High Speed Civil Transport," *Journal of Aircraft*, Vol. 38, No. 6, 2001, pp. 997–1005.

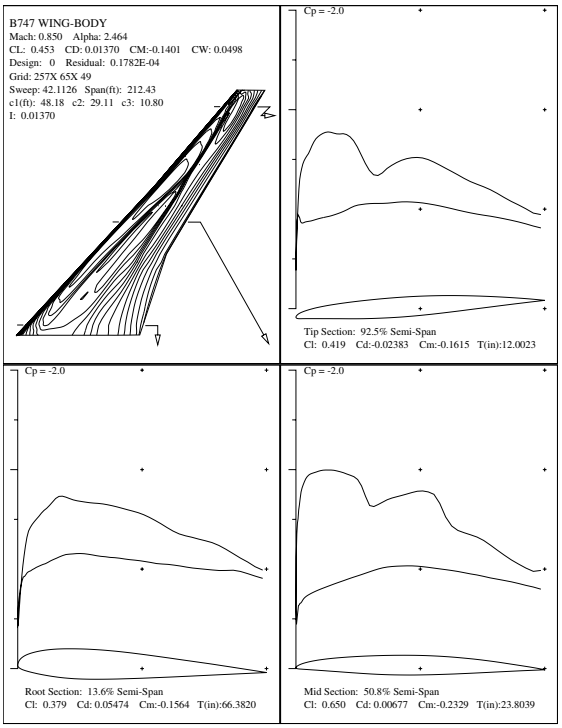

(a) Baseline

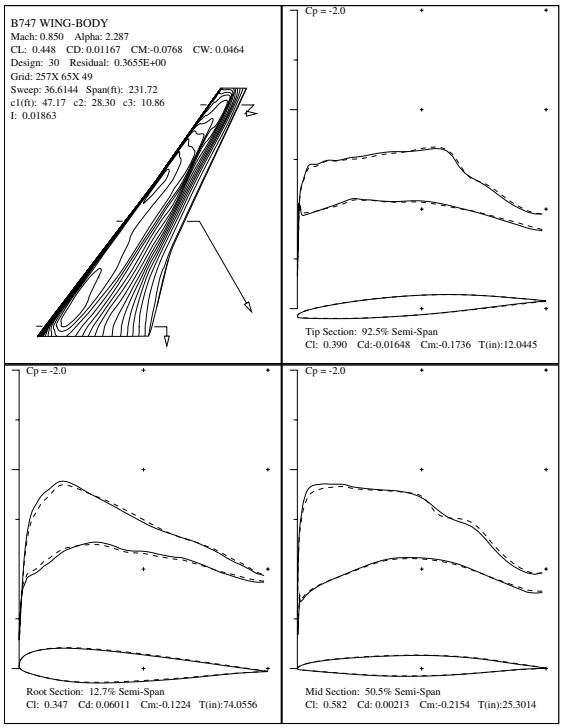

(b) Optimum

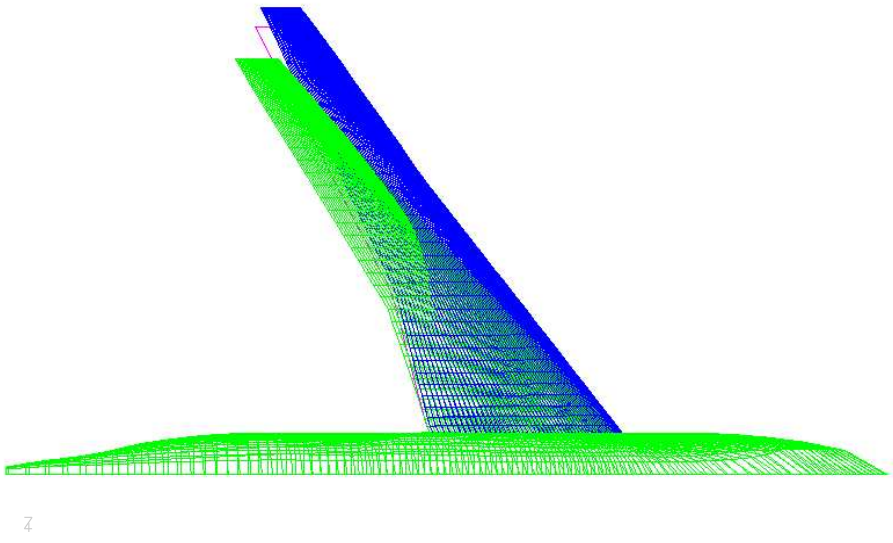

(c) Planform (Baseline : Green, Optimum : Blue)

Figure 4. Redesign of Boeing 747 wing, using section and planform modifications. The optimum wing has longer span, less sweep, and thicker wing sections. We also over-plot the optimum planform form our inviscid calculation[13] to indicate good agreements between the inviscid and viscous optimizations.

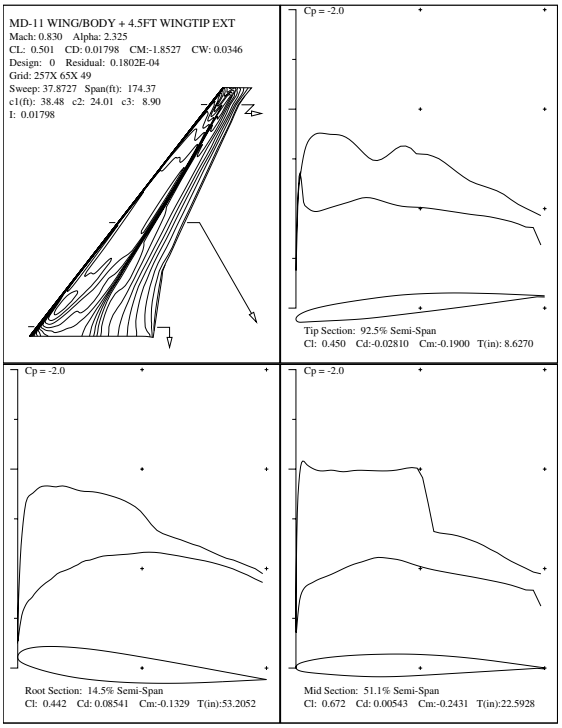

(a) Baseline

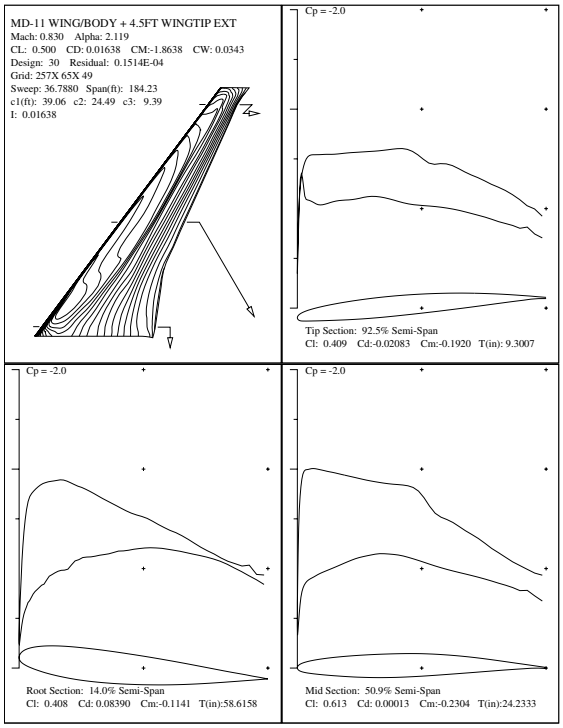

(b) Optimum

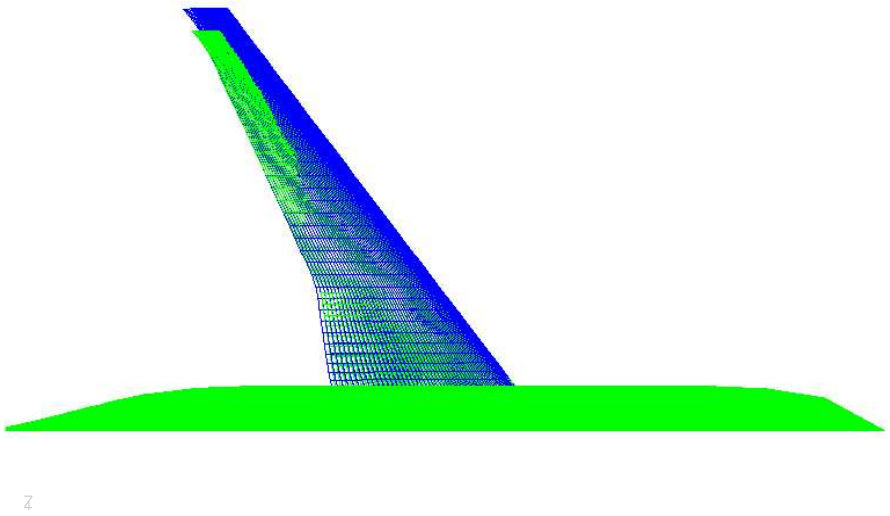

(c) Planform (Baseline : Green, Optimum : Blue)

Figure 5. Redesign of McDonnell Douglas MD 11 wing, using section and planform modifications. The optimum wing has longer span, less sweep, and thicker wing sections.

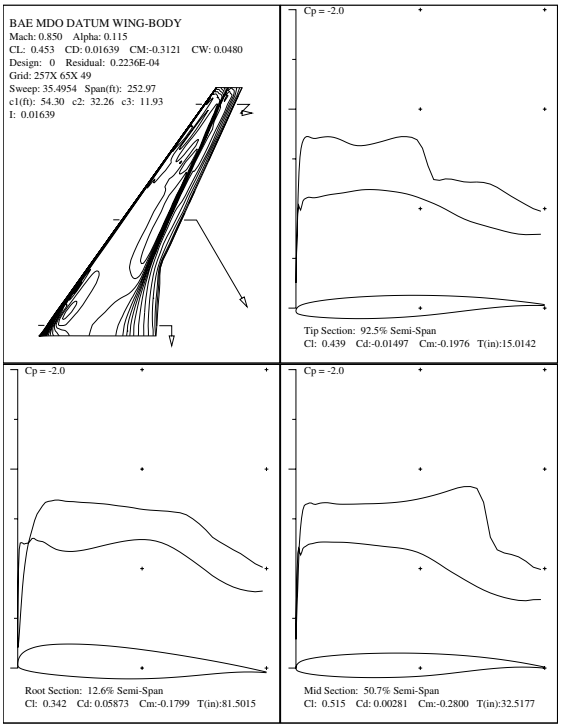

(a) Baseline

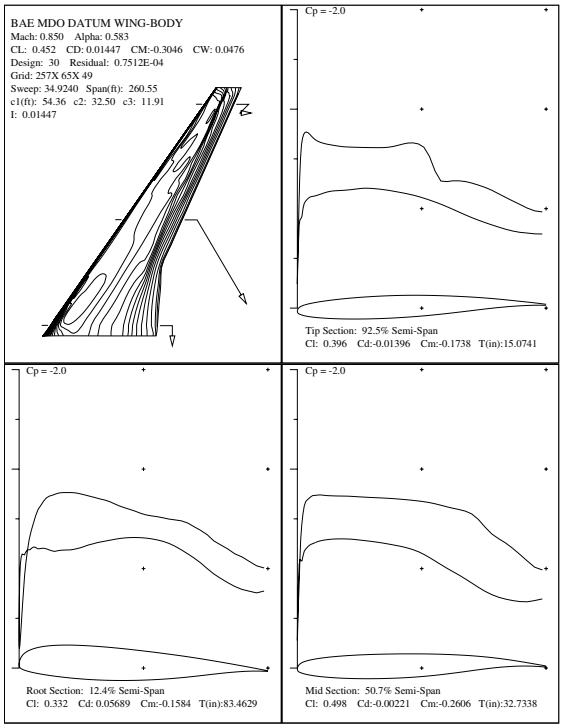

(b) Optimum

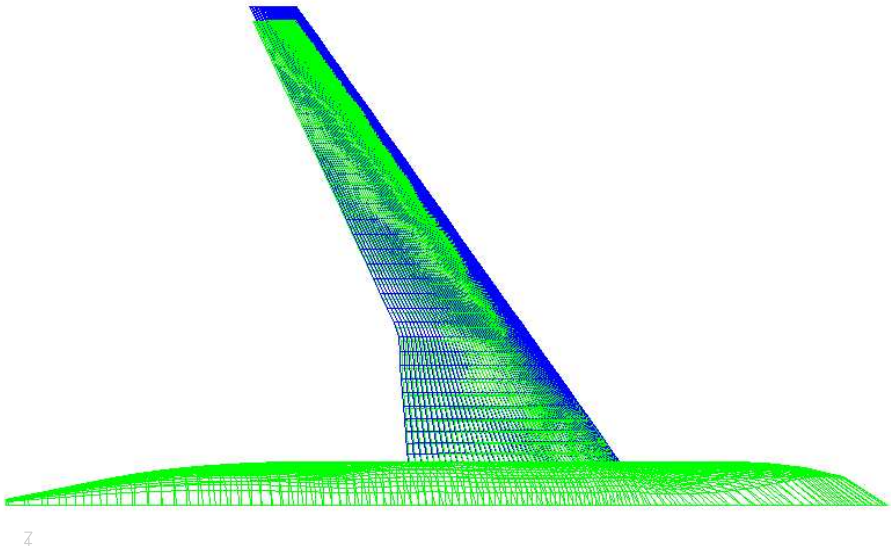

(c) Planform (Baseline : Green, Optimum : Blue)

Figure 6. Redesign of BAe MDO DATUM wing, using section and planform modifications. The optimum wing has longer span, less sweep, and thicker wing sections.

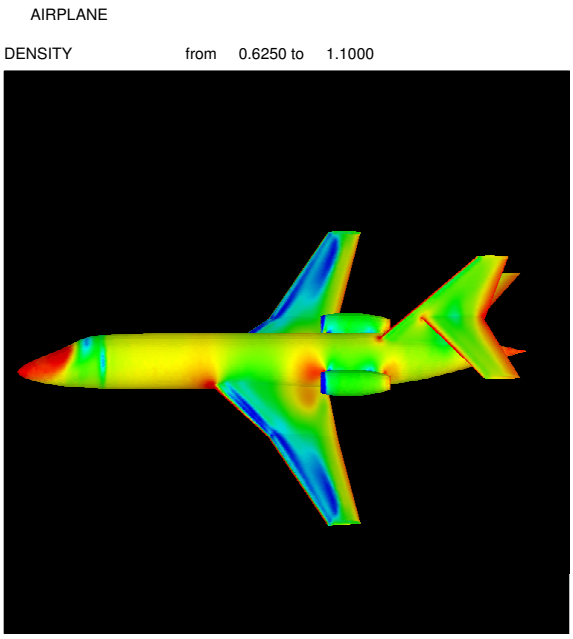

(a) Density contours

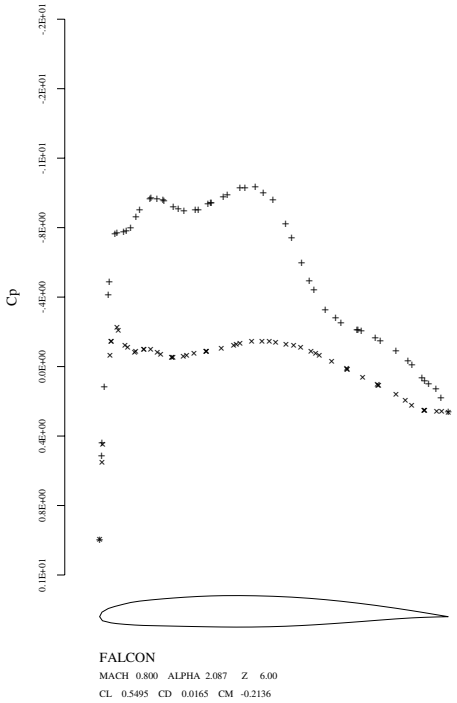

(b) 66 % wing span

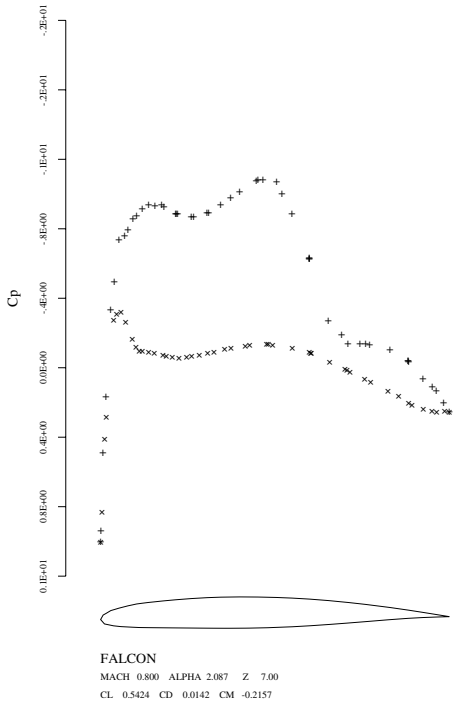

(c) 77 % wing span

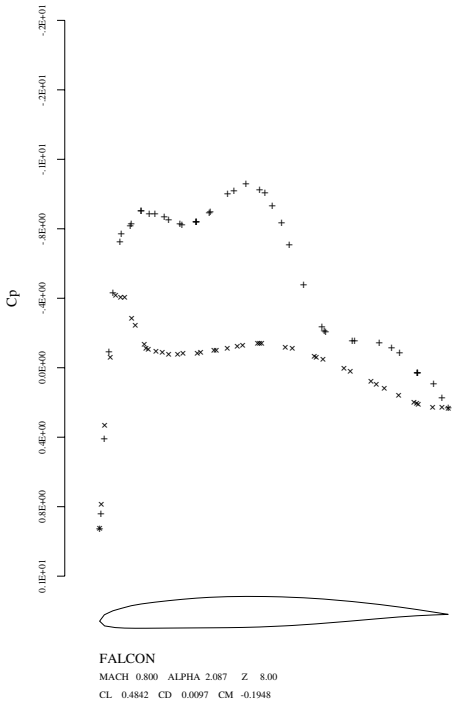

(d) 88 % wing span

Figure 7. A business jet at $M = 0.8$, $\alpha = 2$, baseline

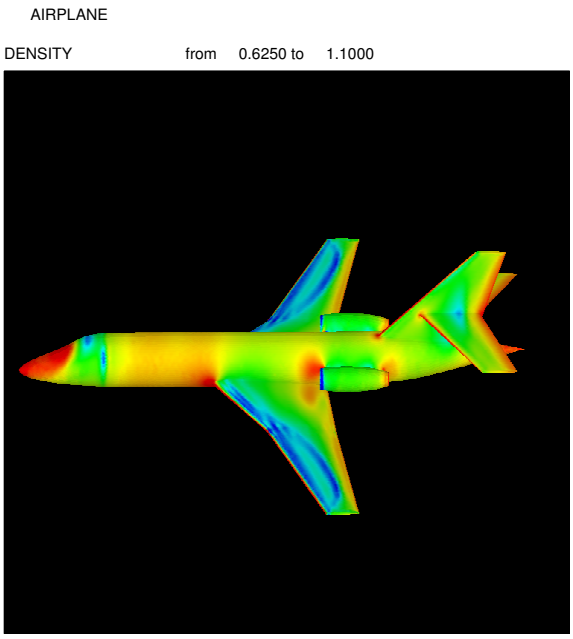

(a) Density contours

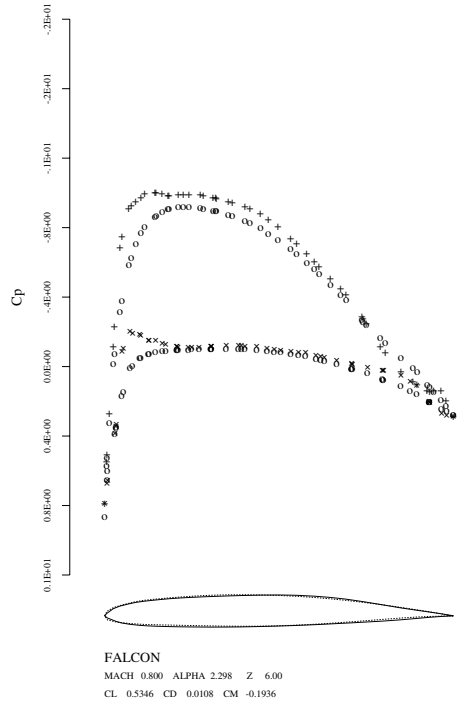

(b) 66 % wing span

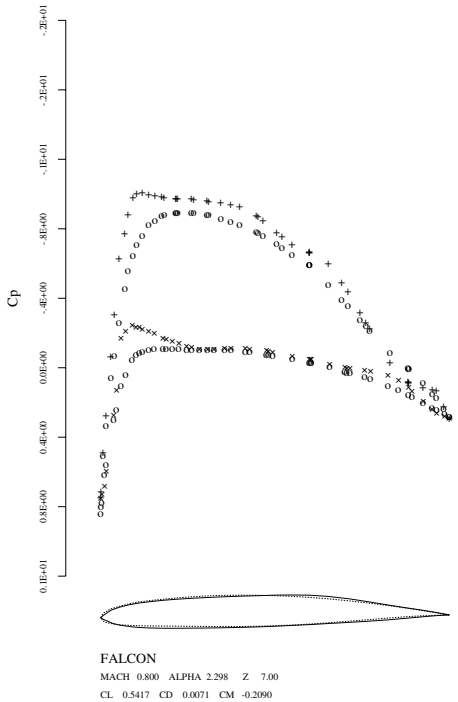

(c) 77 % wing span

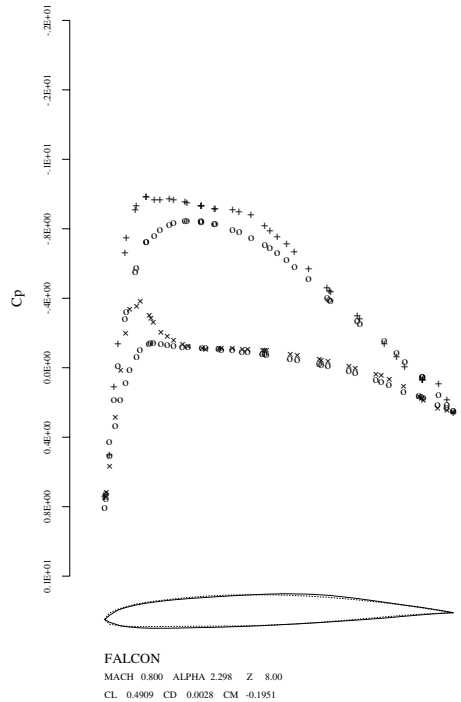

(d) 88 % wing span

Figure 8. A business jet at $M = 0.8$, $\alpha = 2.3$, after redesign

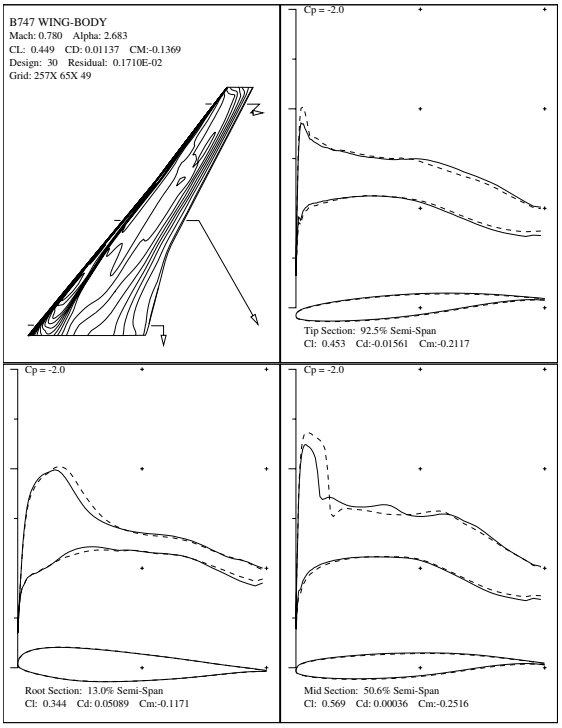

(a) Mach .78

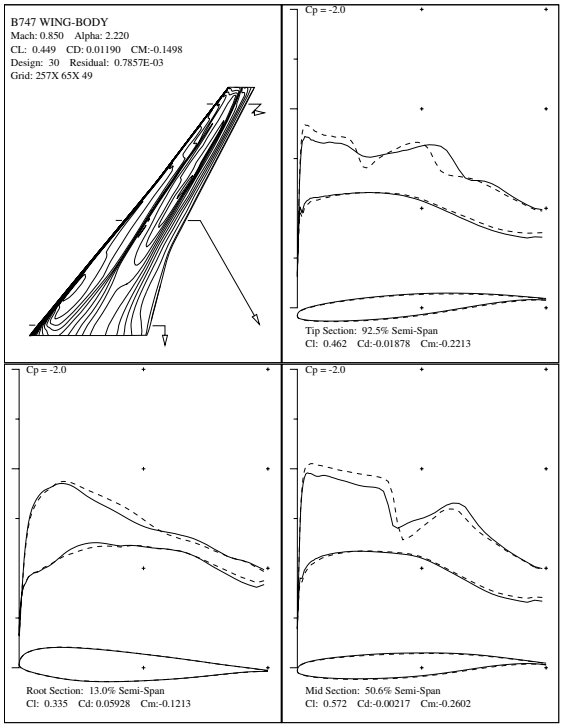

(b) Mach .85

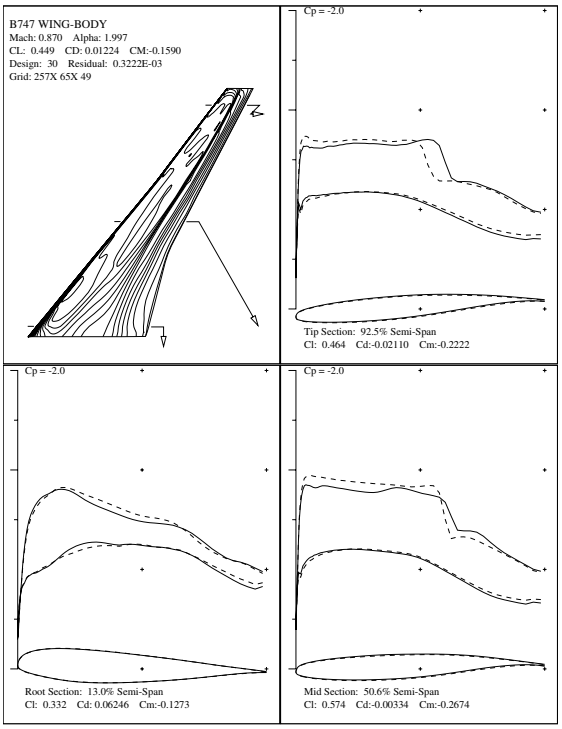

(c) Mach .87

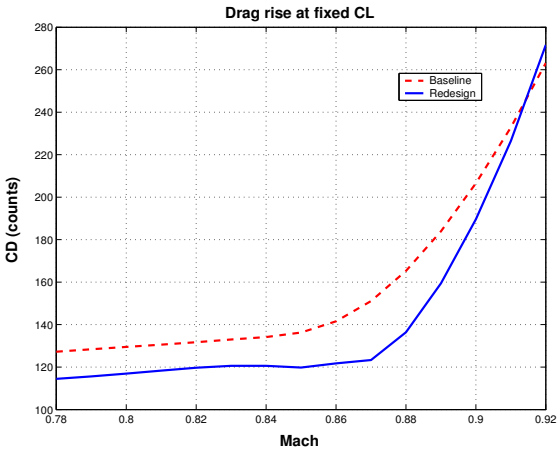

(d) Drag Vs. Mach number

Figure 9. (a)-(c): Super B747 at Mach .78, .85, and .87 respectively. Dash line represents shape and pressure distribution of the initial configuration. Solid line represents those of the redesigned configuration. (d): Drag Vs. Mach number of Super B747.

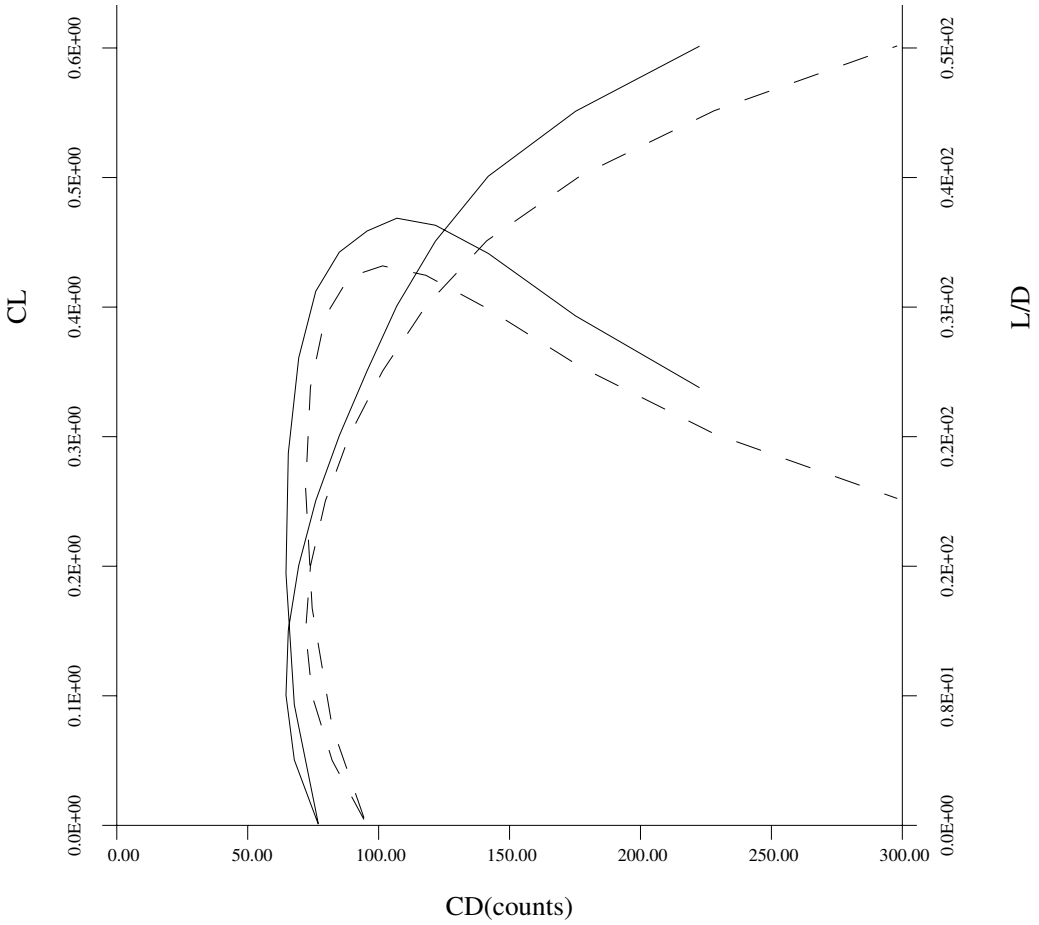

Figure 10. Drag Polars of Baseline and Super B747 at Mach .86. (Solid-line represents Super B747. Dash-line represents Baseline B747.)

Table 2. Comparison of drag polar; B747 Vs. Super B747

Boeing 747		Super B747	
C_L	C_D	C_L	C_D
0.0045	94.3970	0.0009	76.9489
0.0500	82.2739	0.0505	67.8010
0.1000	74.6195	0.1005	64.6147
0.1501	72.1087	0.1506	65.5073
0.2002	73.9661	0.2006	69.4840
0.2503	79.6424	0.2507	76.0041
0.3005	88.7551	0.3008	84.9889
0.3507	101.5293	0.3509	95.6117
0.4009	118.0487	0.4010	106.9625
0.4512	**141.2927**	0.4510	121.7183
0.5014	177.0959	**0.5010**	**141.8675**
0.5516	228.1786	0.5512	175.2569
0.6016	298.0458	0.6014	222.5459

(C_D in counts)

Note the drag-equivalence of the baseline B747 at C_L .45 and the Super B747 at C_L .5.